Available online at www.sciencedirect.com
ScienceDirect
Journal of the European Ceramic Society 29 (2009) 2461–2467
www.elsevier.com/locate/jeurceramsoc

Effect of angled indentation on mechanical properties

Saeed Saber-Samandari [a,b,*], Karlis A. Gross [a,b]

[a] Swinburne University of Technology, Faculty of Engineering and Industrial Sciences, IRIS, Hawthorn, VIC 3122, Australia
[b] Department of Mechanical Engineering, The University of Melbourne, Parkville, VIC 3010, Australia

Received 27 January 2009; received in revised form 4 March 2009; accepted 16 March 2009
Available online 14 April 2009

Abstract

Indentation on a smooth surface, perpendicular to the indenter tip, is critical to obtaining accurate mechanical property values with nanoindentation. However, for some materials, achieving such a scenario may not always be feasible. To investigate the effect this may have, angled indentations were made on flat, sintered hydroxyapatite samples individually mounted so as to produce indentation angles of 10°, 20°, 30°, 40° and 50°, as well as leading contact with either the face or edge of the Berkovich tip used. While significant scatter in results reinforced the importance of perpendicular penetration, two phenomena were found to serve as potential indicators of angled indentation, and hence unreliable data. It is recommended that topographical profiles are obtained on any material of uncertain roughness prior to indentation.

Keywords: Mechanical properties; Nanoindentation; Hydroxyapatite; Rough surface; Tilted sample

1. Introduction

In an ideal nanoindentation experiment, the flat surface of a sample is mounted perpendicular to the tip of the indenter. The tip of the indenter touches the surface of the sample and penetration is performed by applying a known load. Mechanical properties such as hardness and reduced modulus can be obtained from a cycle of loading and unloading.

During an experiment, any phenomenon like pile-up, sink-in, angled indentation or indentation on a rough surface may alter these recorded mechanical properties. Several investigations have been reported on the effect of pile-up and sink-in.[1,2] Other studies have explored the effect of performing indentation on a rough sample.[3–8] The effect of roughness on the hardness value obtained has been found to be negligible if the depth of indentation is much greater than the surface roughness.[9] Thus, producing an approximately flat surface for indentation will minimise the scatter in a measurement. However, some material surfaces are not flat and are dictated by the manufacturing process.

Kim et al. modified an existing indentation size effect (ISE) model to account for work done in flattening a rough surface during indentation.[10] Others have explored using surface roughness corrections or, alternatively, a threshold criterion to deal with roughness issues for certain material types.[11–13] While a majority of these studies have utilised sharp indenters, a relationship between surface roughness and measured mechanical properties has also been reported for spherical indenters[14].

It has been found that thermally sprayed hydroxyapatite (HAp) coatings are not completely flat, but composed of flattened solidified droplets. HAp coating is one example of an aforementioned material for which obtaining a flat surface may not be practicable. The implant surface implanted into the body remains unpolished, and so there is a need to directly evaluate the as-sprayed HAp coated implant surface. Furthermore, the polishing process necessarily involves introducing water to the specimen, which may alter its microstructure and hence its mechanical properties due to its sensitivity to moisture.

Roughness and waviness of thermally sprayed HAp coatings will lead to scatter in nanoindentation data, largely dependent on the position of indentation. It may arise that contact occurs between the sample and a face or edge of the indenter, rather than the indenter tip. The principles of the nanoindentation technique may not be correctly applied in such cases,[15,16] with inaccuracies arising from the incorrectly measured projected area. Though some work has been conducted into effects of the indenter geom-

* Corresponding author at: Swinburne University of Technology, Faculty of Engineering and Industrial Sciences, IRIS, Hawthorn, VIC 3122, Australia. Tel.: +61 3 9214 4345; fax: +61 3 9214 5050.
E-mail address: ssabersamandari@swin.edu.au (S. Saber-Samandari).

0955-2219/$ – see front matter © 2009 Elsevier Ltd. All rights reserved.
doi:10.1016/j.jeurceramsoc.2009.03.010

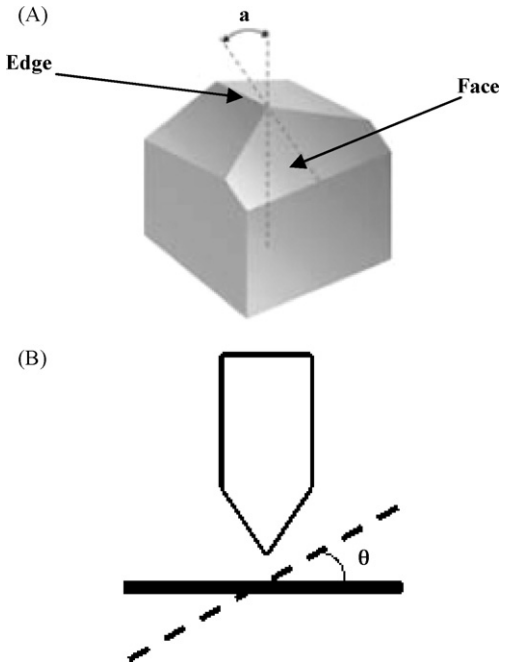

Fig. 1. Schematic image of (A) the Berkovich indenter with face angle of $a = 65.3^\circ$ and (B) position of indenter and sample. Angle θ varies from 0 (solid line) to 50 (dotted line) degrees.

etry (shape and acuity) on a material's mechanical response and measured properties,[17–20] no research has been reported on the effect of angled indentation.

This study is concerned with the slopes that may be found on undulating surfaces, a factor that is present with solidified droplets. A prior investigation has revealed that hardness and modulus values obtained from thermally sprayed HAp coatings were influenced by indentation position.[21] The cause of the variation in the measurement is attributed to the nature of the surfaces. The present study will determine the reduced modulus and hardness of sintered HAp samples at increasing set angles to the indenter. The change in the loading–unloading curves will be shown as a function of the indentation angle.

2. Experimental procedure

A disk shape of HAp sintered at 1200 °C from the prior study[22] was mounted on five different wedges to create indentation angles of 10°, 20°, 30°, 40° or 50°. The surface contact is first established at a known angle to either a face or edge of the indenter. Fig. 1A illustrates the geometry of the Berkovich indenter, which is used in this study. Position of the indenter perpendicular to the surface and tilted surface from 0° to 50° is depicted in Fig. 1B.

2.1. Micromechanical testing

Nanoindentation was performed using a Nano Test instrument (Micro Materials Ltd. Wrexham, UK). It is a pendulum-based depth-sensing system, with the sample mounted horizontally and the load applied electromagnetically. Both the machine and the indenter must be calibrated before any real experiment. To this end, indentations were carried out on a fused silica (FS) specimen. For the reference sample, load-controlled, load–partial-unload experiments of twenty cycles at different depths were performed. Other experimental conditions were preset: loading and unloading rate of 6 mN s^{-1} and 30 s hold for thermal drift correction.

Hardness (H) and reduced modulus (E_r) were determined by the following equations:

$$H = \frac{P_{max}}{A}$$

$$E_r = \frac{1}{\beta}\frac{\sqrt{\pi}}{2}\frac{S}{\sqrt{A}}$$

where P_{max} is the maximum load applied to the projected contact area, A. β is a correction factor depending on the type of indenter used, and takes a value of 1.034 for the Berkovich indenter used in this study. S is the elastic contact stiffness.

Approximately 5 indentations were made on each wedge by applying a 100 mN load. Constant hardness at larger loads and higher hardness values (ISE) at loads less than 100 mN were observed.[23] The loading/unloading rate of 10 mN s^{-1} was selected. The dwell period for thermal drift correction was set to 60 s. The initial load was set to 0.1 mN. A set of indentations was made for both face and edge surface contacts.

2.2. Surface morphology

The 2-D profile of thermally sprayed HAp was determined using an XP-2 High Resolution Surface Profilometer, Ambios Technology, Inc., CA, USA.

After performing nanoindentation on the surface of the sintered HAp sample, Scanning Electron Microscopy (SEM) was used to observe the residual impression at high magnification with a larger depth of focus than achievable with an optical microscope. The morphology of the impression was then examined using an XL30 Philips SEM with an accelerating voltage of 20 keV. Samples were sputter coated with gold before examination in the SEM.

3. Results and discussion

An indentation conducted perpendicular to the surface ($\theta = 0^\circ$) provided an equilateral triangular indent, Fig. 2. The loading–unloading curve follows the typical shape of the loading indicating a higher resistance to deformation with increasing depth. The SEM image shows no evidence of cracking during indentation into the sintered HAp. Also noted is the clean, symmetric nature of the impression reflecting the symmetrical geometry of the indenter tip. Under the applied 100 mN load, hardness and reduced modulus were found to be 7.1 ± 0.3 and 116.7 ± 0.6 GPa, respectively.

For very rough samples, contact may occur at an angle to the indentation direction. The surface of a commercial thermally sprayed HAp coating is mapped in Fig. 3 over a randomly selected 300 μm region. The roughness is seen to be significant, with several droplets discernible along the length. In this sec-

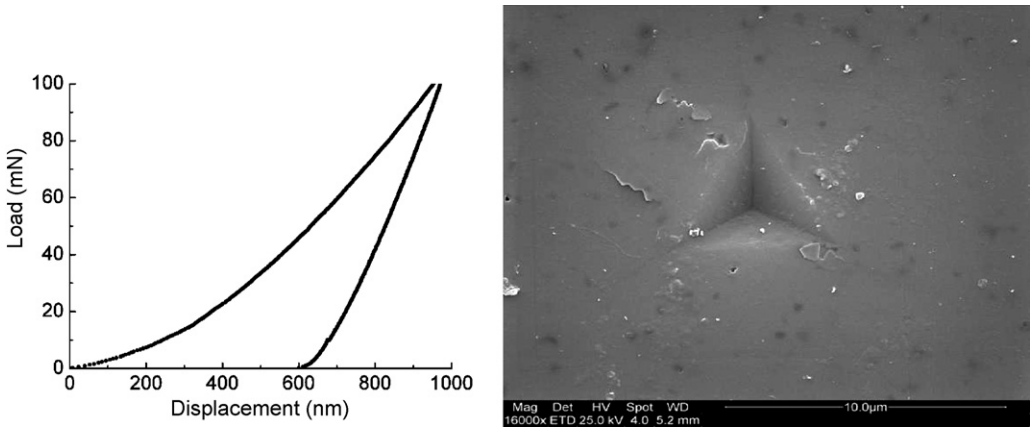

Fig. 2. Load–displacement curve for one cycle of loading and unloading, and the corresponding SEM image of a perpendicular indentation into sintered HAp.

tion alone there is a maximum amplitude difference of ∼15 μm. The variation in height is also very non-uniform, as deposited droplets overlap one another. Indentations blindly performed on a coating could therefore be located on a droplet centre or on the edges or overlapping regions at a range of angles. Furthermore, contact may occur not only with the tip, but with either the face or the edge of the indenter. The inset of Fig. 3 illustrates this concept on the surface profile of a 65 μm diameter single droplet, enlarged from the 300 μm scanned region. The uneven slopes and almost 9 μm displacement from base to top of the droplet provide a range of possible indentation scenarios as indicated. As a result, the projected contact area calculated will be in error, resulting in overestimated or underestimated mechanical properties. To investigate this effect, angled indentations were performed on negligibly rough sintered HAp samples.

Load–displacement curves and residual impression images of nanoindentations which touch the face of the indenter at 10°, 20°, 30° and 40° are shown in Fig. 4. In changing the mounted sample from $\theta = 0°$ to 10°, hardness and reduced modulus dramatically reduce to 2.9 ± 0.8 and 38.3 ± 5.5 GPa, respectively. However, changing from 10° to 20° caused mechanical properties to increase while the residual impression again decreases. This increment in mechanical properties is observed until 30°, after which they drop abruptly. At the angle of 40°, the sample just touches the face of the indenter and a clear indentation was not observed (Fig. 4). From inspection of the load–displacement curves, the final depth reduces from 600 to 50 nm for 0° to 50°, respectively. The depth of penetration shows erratic behaviour, decreasing from 1500 nm at 10° to 1050 nm at 30° and then increasing up to 1890 nm at 50°.

Quite different behaviour is observed for the indenter edge contact, Fig. 5. From $\theta = 0°$ to 10°, mechanical properties increased; hardness and reduced modulus were recorded as 10.4 ± 1.1 and 167.6 ± 7.3 GPa, respectively. These values then decreased continually with angle to 6.7 ± 1.3 and 56.2 ± 5.6 GPa at 30°. Again, a "critical angle", at which the increment in hardness and modulus values change direction, is observed around 30°. It is speculated this may be linked to the indenter geometry, the Berkovich tip (Fig. 1A) having a face angle ($a = 65.3°$) almost the complement of this critical angle. Such a connection remains uncertain, as no experiment at 25° inclination was conducted. The size of the residual impression decreases from 10° to 40°. The final depth remained approximately the same, between 350 and 420 nm, for all angles, as did the depth of penetration, 900 ± 50 nm. Again, this is very different behaviour than that observed for face contact.

No residual impressions could be found for the 50° angle (Fig. 6). The depth of penetration reaches almost 2000 nm for face contact while the edge contact penetrates less than half of that, sitting around the same value as seen for the other angles with this type of contact. Further, edge contact tolerates a 100 mN load, while the face contact indentation stopped at a load of ∼40 mN due to too large a penetration depth. Hardness and reduced modulus of all angles for both face and edge contact are shown in Fig. 7.

These results serve to demonstrate the considerable unreliability of any data obtained on mechanical properties when perpendicular indentations are not produced. This is an issue for materials, such as rapidly solidified HAp, whose microstructure can be altered by polishing processes to achieve the desired flat surface. Flatter HAp coatings could be achieved with control of the droplet temperature and velocity before impact. This would enable the measurement of micromechanical properties by indenting the surface of individual flattened solidified droplets. Nevertheless, it would be useful to know whether nanoindentation data has been influenced by topographical factors.

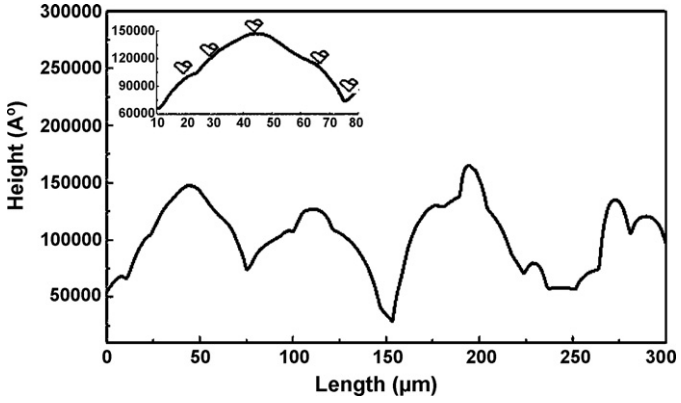

Fig. 3. A 2-D profile of thermally sprayed HAp showing surface roughness.

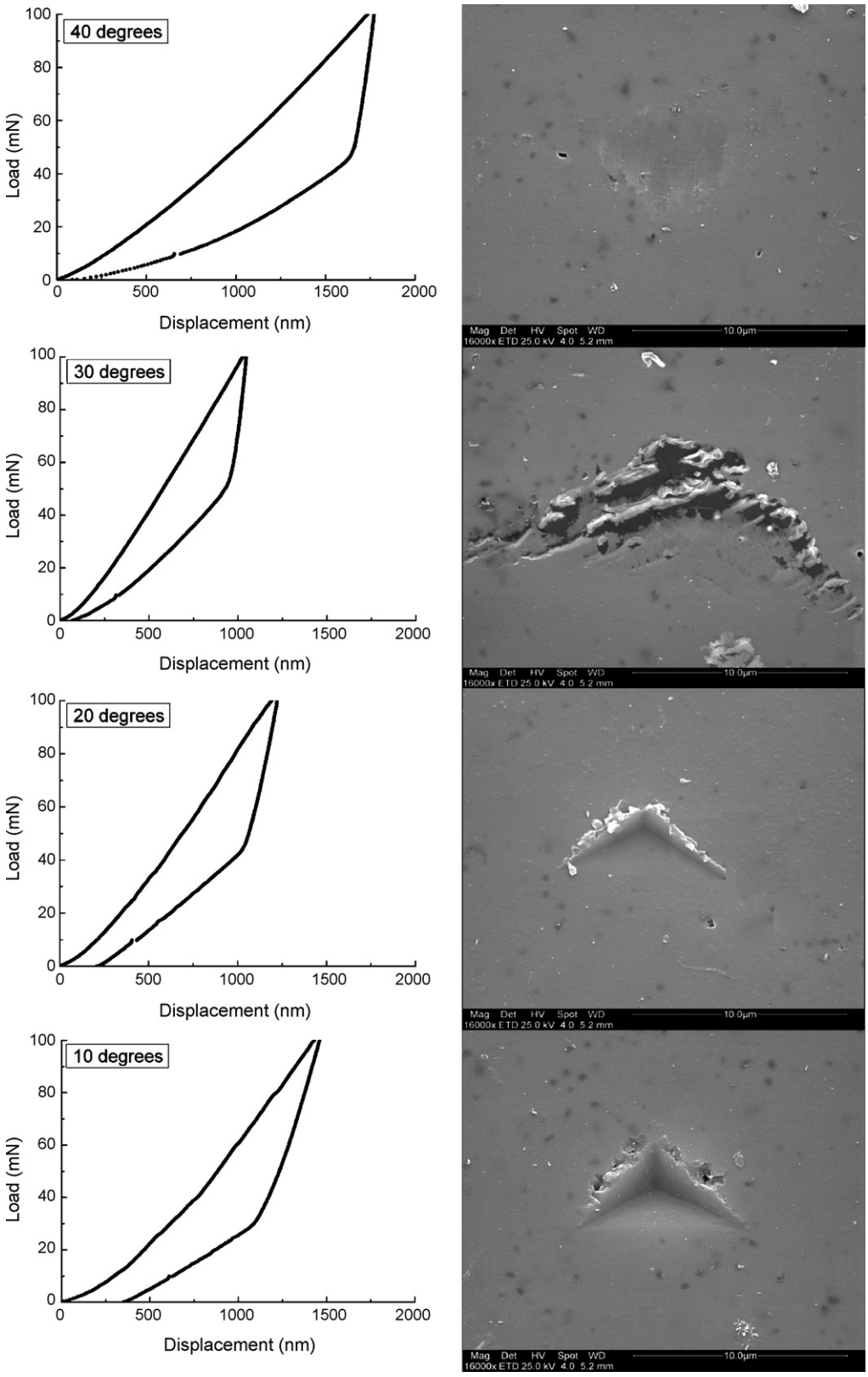

Fig. 4. Load–displacement curves for one cycle of loading and unloading, and the corresponding SEM images for angled face contacts.

To that end, two phenomena are consistently observed for all non-perpendicular indentations. One is the non-symmetrical appearance of the residual impressions in the SEM images. This is a direct result of the surface orientation and unbalanced face or edge contact. The other is the elbow (change in slope) in the unloading portion of each load–displacement curve. Nanoindentation experiments on silicon have reported elbows in unloading curves caused by phase transformations under certain loading

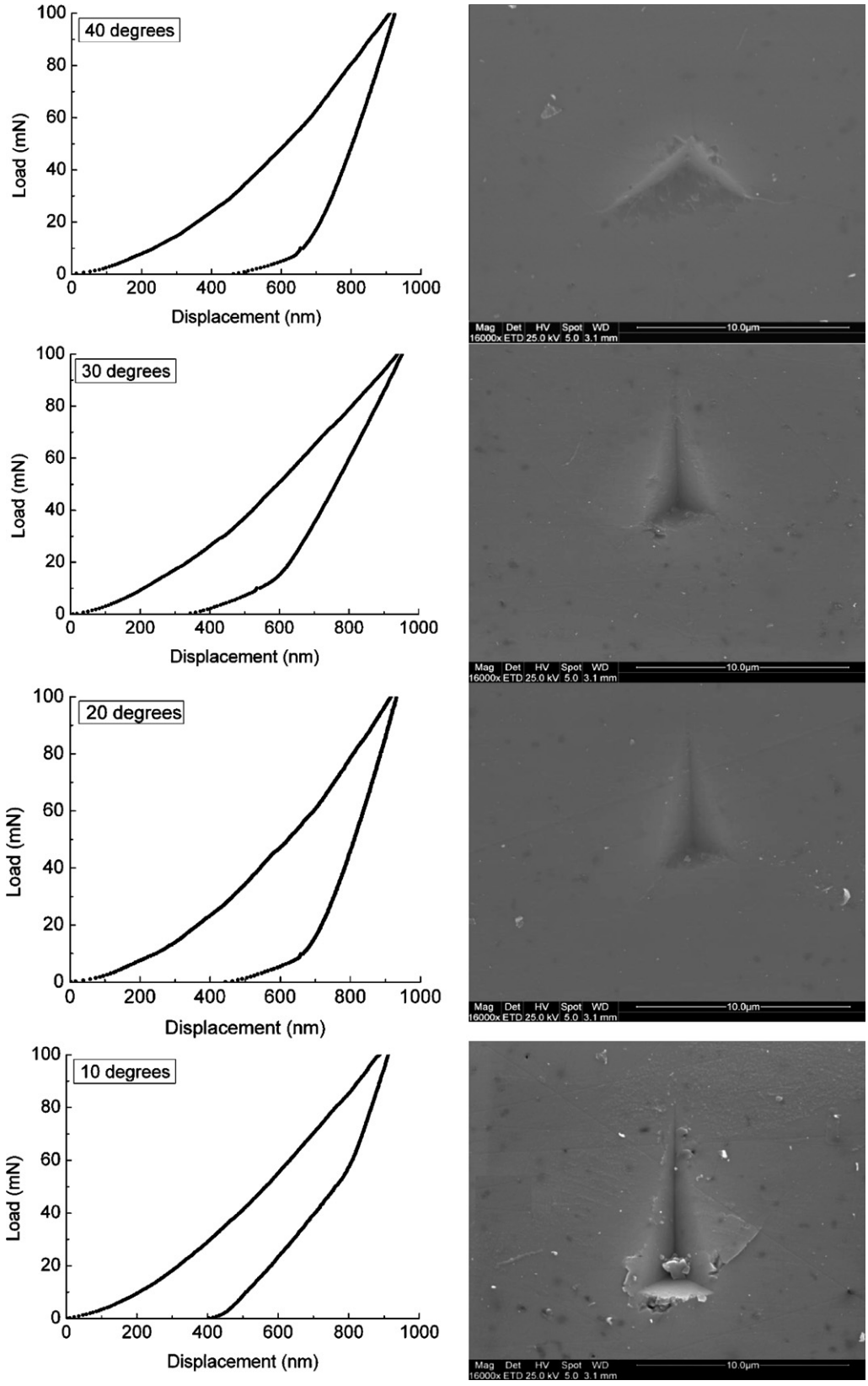

Fig. 5. Load–displacement curves for one cycle of loading and unloading, and the corresponding SEM images for angled edge contacts.

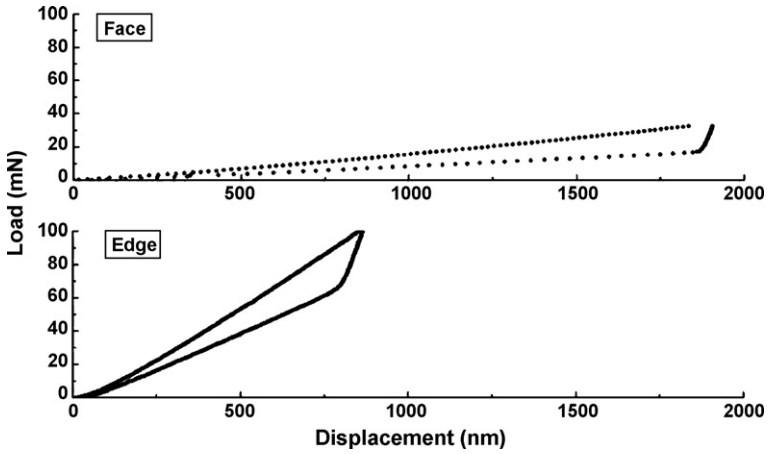

Fig. 6. Load–displacement curves for a single loading–unloading cycle at the angle of 50° for both face and edge contact (no residual indentation found with the SEM).

conditions.[24,25] However, the lack of an elbow event in the unloading curve for the perpendicular indentation, given the identical experimental settings applied in all tests, suggests a different source for this occurrence of the phenomenon. It is the authors' conjecture that these elbow events are a result of angled indentations, and the associated asymmetric loading of the indenter tip. This is further supported by the slightly sharper elbows for larger indentation angles.

Such information would be beneficial for future nanoindentation studies, particularly on materials with a greater level of roughness. The observation of asymmetric residual impressions under the microscope would be a clear indicator that indentation did not occur perpendicular to the surface. However, if SEM imaging is not available, one could simply inspect the unloading curves for elbow events. The appearance of both phenomena would be very telling evidence that angled indentation has occurred, and therefore the accuracy of any calculated mechanical properties are not reliable.

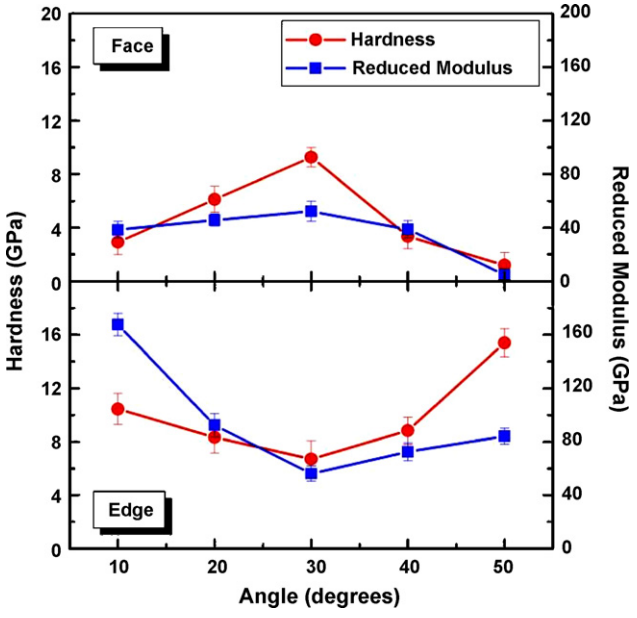

Fig. 7. Hardness and reduced modulus vs. angle for both edge and face contacts. Note that hardness and reduced modulus at 0° (perpendicular) was found to be 7.03 and 116.74 GPa, respectively.

4. Conclusions

The effect of indenter penetration angle on micromechanical properties was comprehensively studied. Indentations on sintered HAp samples were performed, while the sample was tilted at angles of 10°, 20°, 30°, 40° and 50°. An angle around 30° was determined to be a "critical angle", which may be related to the geometry of the indenter. Coexistent asymmetric residual impressions and elbow events in unloading curves have been attributed to the non-perpendicular surface penetration of the indenter tip. The observation of either of these phenomena should serve as an indicator of an angled indentation that produces incorrect mechanical property values.

Acknowledgements

The authors acknowledge support from an ARC project # DP0774251. The nanoindentation instrument was purchased with funds provided by the Rowden White Fund and supplemented by the ARC LIEF grant # LE0775715. The authors would like to thank Ms. Karina S. Heemann for her help in preparing the manuscript.

References

1. Bolshakov, A. and Pharr, G. M., Influences of pileup on the measurement of mechanical properties by load and depth sensing indentation techniques. *J. Mater. Res.*, 1998, **4**, 1049–1058.
2. Pharr, G. M. and Bolshakov, A., Understanding nanoindentation unloading curves. *J. Mater. Res.*, 2002, **17**, 2660–2671.
3. Bobji, M. S. and Biswas, S. K., Estimation of hardness by nanoindentation of rough surfaces. *J. Mater. Res.*, 1998, **13**, 3227–3233.
4. Shibutani, Y. and Koyama, A., Surface roughness effects on the displacement bursts observed in nanoindentation. *J. Mater. Res.*, 2004, **19**, 183–188.
5. Donnelly, E., Baker, S. P., Boskey, A. L. and Meulen, M. C. H., Effects of surface roughness and maximum load on the mechanical properties of cancellous bone measured by nanoindentation. *J. Biomed. Mater. Res.*, 2006, **77A**, 426–435.

6. Jiang, W. G., Su, J. J. and Feng, X. Q., Effect of surface roughness on nanoindentation test of thin films. *Eng. Fract. Mech.*, 2008, **75**, 4965–4972.
7. Zhang, T.-Y., Xu, W.-H. and Zhao, M.-H., The role of plastic deformation of rough surfaces in the size-dependent hardness. *Acta Mater.*, 2004, **52**, 57–68.
8. Wei, Y., Wang, X. and Zhao, M., Size effect measurement and characterization in nanoindentation test. *J. Mater. Res.*, 2004, **19**, 208–217.
9. Tabor, D., *The Hardness of Metals*. Clarendon Press, Oxford, United Kingdom, 1951.
10. Kim, J. Y., Kang, S. K., Lee, J. J., Jang, J. I., Lee, Y. H. and Kwon, D., Influence of surface-roughness on indentation size effect. *Acta Mater.*, 2007, **55**, 3555–3562.
11. Grau, P., Ullner, C. and Behncke, H.-H., Uncertainty of depth sensing hardness. *Materialpruefung*, 1997, **39**, 362–367.
12. Bobji, M. S. and Biswas, S. K., Deconvolution of hardness from data obtained from nanoindentation of rough surfaces. *J. Mater. Res.*, 1999, **14**, 2259–2268.
13. Miller, M., Bobko, C., Vandamme, M. and Ulm, F. J., Surface roughness criteria for cement paste nanoindentation. *Cem. Conc. Res.*, 2008, **38**, 467–476.
14. Walter, C., Antretter, T., Daniel, R. and Mitterer, C., Finite element simulation of the effect of surface roughness on nanoindentation of thin films with spherical indenters. *Surf. Coat. Technol.*, 2007, **202**, 1103–1107.
15. Doerner, M. F. and Nix, W. D., A method for interpreting the data from depth-sensing indentation instruments. *J. Mater. Res.*, 1986, **1**, 601–609.
16. Oliver, W. C. and Pharr, G. M., An improved technique for determining hardness and elastic modulus using load and displacement sensing indentation experiments. *J. Mater. Res.*, 1992, **7**, 1564–1583.
17. Hay, J. C., Bolshakov, A. and Pharr, G. M., A critical examination of the fundamental relations used in the analysis of nanoindentation data. *J. Mater. Res.*, 1999, **14**, 2296–2305.
18. Warren, A. W. and Guo, Y. B., Machined surface properties determined by nanoindentation: experimental and FEA studies on the effects of surface integrity and tip geometry. *Surf. Coat. Technol.*, 2006, **201**, 423–433.
19. Jang, J. and Pharr, G. M., Influence of indenter angle on cracking in Si and Ge during nanoindentation. *Acta Mater.*, 2008, **56**, 4458–4469.
20. Morris, D. J., Myers, S. B. and Cook, R. F., Sharp probes of varying acuity: instrumented indentation and fracture behavior. *J. Mater. Res.*, 2004, **19**, 165–175.
21. Gross, K. A. and Saber-Samandari, S., Nano-mechanical properties of hydroxyapatite coatings with a focus on the single solidified droplet. *J. Aust. Ceram. Soc.*, 2007, **43**, 98–101.
22. Gross, K. A. and Rodríguez-Lorenzo, L. M., Sintered hydroxyfluorapatites. Part I: sintering ability of precipitated solid solution powders. *Biomaterials*, 2004, **25**, 1375–1384.
23. Gross, K. A. and Saber-Samandari, S., Revealing mechanical properties in a hydroxyapatite suspension plasma sprayed coating with nanoindentation. *Surf. Coat. Technol*. (2009), doi:10.1016/j.surfcoat.2009.03.007.
24. Domnich, V., Gogotsi, Y. and Dub, S., Effect of phase transformations on the shape of the unloading curve in the nanoindentation of silicon. *Appl. Phys. Lett.*, 2000, **76**, 2214–2216.
25. Juliano, T., Gogotsi, Y. and Domnich, V., Effect of indentation unloading conditions on phase transformation induced events in silicon. *J. Mater. Res.*, 2003, **18**, 1192–1201.